Feasibility of the Inoue single-branched stent-graft implantation for thoracic aortic aneurysm or dissection involving the left subclavian artery: Short- to medium-term results in 17 patients

Naritatsu Saito, MD,[a] Takeshi Kimura, MD,[a] Keita Odashiro, MD,[b] Masanao Toma, MD,[a] Masakiyo Nobuyoshi, MD,[b] Katsuya Ueno, RT,[c] Toru Kita, MD,[a] and Kanji Inoue, MD,[d]
Kyoto and Kokura, Japan

Objective: This study assessed the short- to medium-term clinical results of the Inoue single-branched stent graft for repair of thoracic aortic aneurysms or dissections involving the left subclavian artery.
Methods: A retrospective review of experiences at two institutions was performed. We analyzed the data of consecutive 17 patients with thoracic aortic aneurysms or dissections who underwent endovascular repairs with the Inoue single-branched stent graft between July 1999 and April 2004. Complete baseline and follow-up data were available on all patients. The mean age was 71 ± 9 years, and 13 of the patients (76%) were men. Eight patients (47%) were considered unfit for open surgery because of advanced age or the presence of comorbid diseases.
Results: The stent grafts were successfully delivered and deployed in all 17 patients. Periprocedural major complications, defined as those that caused any persistent disorder, occurred in one patient who developed spinal ischemia. A postoperative computed tomographic scan revealed three attachment site endoleaks; two endoleaks were from the proximal attachment sites and one endoleak was from the distal attachment site. The mean follow-up period was 26 months (range, 7 to 65 months). Two deaths occurred in the follow-up period from cerebral bleeding and pneumonia, both considered unrelated to the stent grafting. Two patients with attachment site endoleaks needed secondary stent-grafting; one patient required the implantation of a straight stent-graft in the distal attachment site and the other, the implantation of a double-branched stent-graft. Another patient with attachment site endoleak was considered very high-risk for open surgery or secondary stent grafting and did not undergo secondary intervention. The aneurysmal sac size of the patient has been stable for 28 months. The branched section of the stent graft was patent in all patients in the follow-up period.
Conclusion: The results demonstrate the feasibility of the Inoue single-branched stent graft for thoracic aortic aneurysms or dissections involving the left subclavian artery. (J Vasc Surg 2005;41:206-12.)

Open surgical repair is considered the traditional treatment for patients with thoracic aortic aneurysms. Despite recent advances in surgical techniques and anesthetic management, the surgical repair of thoracic aortic aneurysms is still associated with significant mortality and morbidity.[1] Endovascular stent grafting of thoracic aortic aneurysms is emerging as an alternative method for repair in selected patients.[2,3] Although endovascular stent grafting is less invasive than open surgical procedures, involvement of branch vessels in the aortic arch limits the application of stent grafting.

From the Department of Cardiovascular Medicine, Graduate School of Medicine, Kyoto University[a]; Department of Cardiology, Kokura Memorial Hospital[b]; and Department of Radiology[c] and Department of Cardiovascular Surgery,[d] Takeda Hospital.

Competition of interest: Dr Kanji Inoue holds all patents of the Inoue stent graft, which was developed and made by Dr Inoue. Dr Kanji Inoue is the only author who holds patents of the stent graft.

Reprint requests: Naritatsu Saito, MD, Department of Cardiovascular Medicine, Graduate School of Medicine, Kyoto University, 54 Shogoin, Sakyo-ku, Kyoto 606-8507, Japan; (e-mail: naritatu@kuhp.kyoto-u.ac.jp).

0741-5214/$30.00

doi:10.1016/j.jvs.2004.11.030

Thoracic aortic aneurysms that involve the left subclavian artery are not rare. In the combined results of the EUROSTAR and the United Kingdom Thoracic Endograft registries, it was necessary to place a stent graft over the left subclavian artery in 17% of the patients.[4] Thurnher et al[5] reported that they required subclavian artery transposition in 24% of their cases.

Our method of managing the left subclavian artery is to provide a stent graft with a side branch. This method does not require the surgical revascularization of the left subclavian artery. This study assessed the short- to medium-term clinical results of Inoue single-branched stent-graft implantations for thoracic aortic aneurysms involving the left subclavian artery.

METHODS

Patients. Between July 1999 and April 2004, endovascular grafting with the Inoue single-branched stent graft was undertaken in 17 patients with thoracic aortic aneurysms or dissections at Kokura Memorial Hospital, Kokura and Kyoto University Hospital, Kyoto, Japan. All patients gave their informed consent in conformance with the protocols approved by the institutional review board of each

Table I. Demographics and comorbidities of the patients

Patients	*Sex*	*Age*	*Etiology*	*Maximum diameter of aneurysm (mm)*	*Unfit for open surgery*	*Risk of open surgery*
No. 1	M	77	degenerative	50	No	
No. 2	F	66	aneurysmal degeneration of a long standing aortic dissection	64	No	
No. 3	M	60	chronic aortic dissection	60	No	
No. 4	M	48	chronic aortic dissection	47	No	
No. 5	M	81	aneurysmal degeneration of a long standing aortic dissection	62	Yes	Advanced age*
No. 6	M	69	acute aortic dissection	46	No	
No. 7	M	80	degenerative	61	Yes	Advanced age
No. 8	M	79	degenerative	75	No	
No. 9	M	75	chronic aortic dissection	70	No	
No. 10	M	67	degenerative	68	Yes	Cerebrovascular disease Prior thoracotomy
No. 11	M	73	degenerative	43	No	
No. 12	M	66	acute aortic dissection	39	Yes	Traumatic injury (rib fracture)
No. 13	—	74	degenerative	50	Yes	Lung disease
No. 14	F	71	degenerative	56	No	
No. 15	M	81	degenerative	70	Yes	Advanced age
No. 16	M	70	degenerative	60	Yes	Lung disease
No. 17	F	78	Ductus diverticulum	68	Yes	Lung disease

F = female; *M* = male.
*Advanced age was defined as over 79 years.

hospital. The mean age was 71 ± 9 years, and 13 patients (76%) were men. Eight patients (47%) were considered unfit for conventional surgical repair because of advanced age or the presence of comorbid diseases. The remaining nine patients rejected open surgery and strongly preferred endovascular repair.

The etiologies of the aneurysms were atherosclerotic aneurysms in nine patients, chronic dissecting aneurysms with patent false lumens in four patients, aneurysmal degeneration of long-standing aortic dissections with thrombosed false lumens in two patients, one traumatic acute aortic dissection, and one aneurysm of the ductus diverticulum.

The Inoue single-branched stent graft was placed into the distal aortic arch, including the origin of the left subclavian artery and the descending aorta. The proximal and distal landing zones required at least 10 mm in length. The front part of the proximal landing zone was at least 5 mm distal to the left common carotid artery. The mean diameter of the aneurysms was 58 ± 11 mm. The demographics and comorbidities of the patients are presented in Table I. Complete baseline and follow-up data are available on all patients.

Device. The Inoue endovascular grafting system consists of a stent graft, a detachable carrying wire, two detachable traction wires, a balloon catheter, and an introducer sheath (Fig 1). The size of the introducer sheath was determined individually, but was usually 20F to 24F.

The Inoue stent graft is constructed from a woven Dacron polyester fabric cylinder. The outside surface of the stent graft is supported with multiple rings of extra-flexible nickel titanium wire covered by Dacron filaments. Small Dacron cuffs are attached to the first and second rings from each end to improve the sealing function. The Inoue single-branched stent graft consists of an aortic section and a branched section. The aortic section and the branched section are sewn together.

The Inoue stent grafts were custom made. We used a specialized computer system for designing the Inoue stent graft.[6] A three-dimensional model was constructed from helical computed tomography (CT) images for the aneurysm. The stent graft was designed and positioned endoluminally on the computer (Fig 2). The diameter and length of each section of the stent graft was determined for each patient. The diameter of the aortic section of the graft was usually oversized by 2 mm and the branched section by 1 mm to achieve effective sealing. The ring of nickel titanium wire attached to the graft was oversized by more than 2 mm.

Each section of the stent graft was individually folded using loops of thread and nickel titanium wire. By removing the nickel titanium wire, each section of the stent graft was unfolded. Three detachable wires were also attached to the stent graft. A carrying wire was attached to the proximal end of the aortic section, and a traction wire was attached to the distal end of the aortic section. Another traction wire was attached to the branched section. The Inoue stent graft was delivered through the introducer sheath with the aid of the carrying and traction wires. A large compliant balloon was used in the dilatation of the aortic graft section. The balloon was custom made and inserted via the introducer sheath (Fig 1).

Implantation technique. All 17 procedures were performed in the cardiac catheterization laboratory under local anesthesia. The patient's femoral artery was surgically iso-

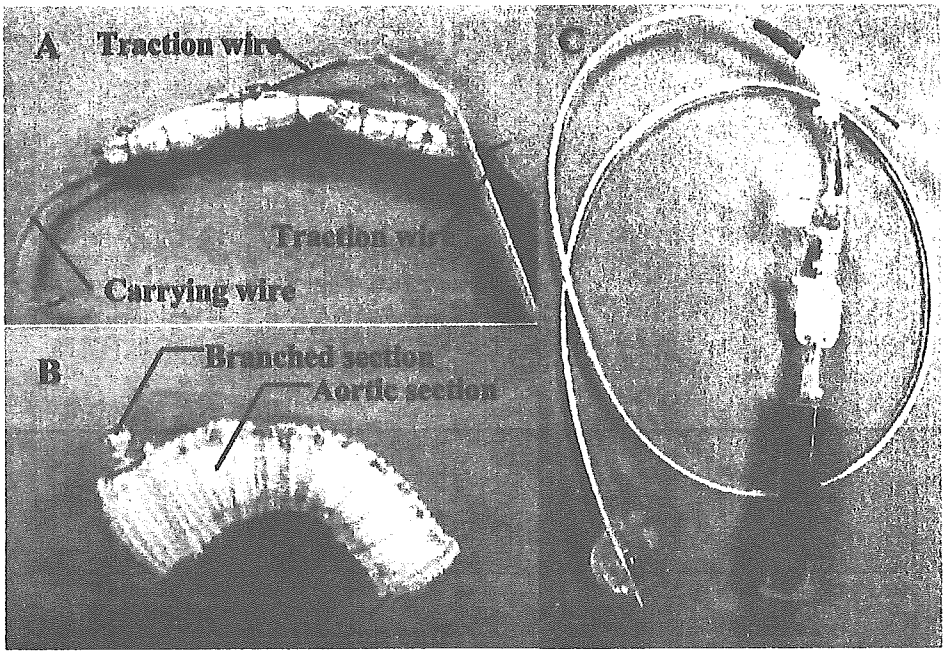

Fig 1. The Inoue single branched stent-graft (*A* and *B*) and the balloon (*C*). A. The folded state. The carrying wire is attached to the proximal end of the aneurysm. Each traction wire is attached to the branched section and the aortic section. B. The unfolded state. The stent-graft consists of the aortic section and the branched section.

lated and a transverse arteriotomy performed. A 7F sheath was inserted percutaneously in the left brachial artery. The introducer sheath was inserted through the femoral artery and advanced to the descending thoracic aorta under fluoroscopic guidance. After administration of 10000 U of heparin, the folded stent graft was introduced into the sheath, advanced to the descending thoracic aorta, and released from the sheath. The folded graft was then pushed to the distal aortic arch.

A 7F catheter with a gooseneck wire was inserted through the 7F sheath in the left brachial artery. The free end of the traction wire attached to the tip of the branched graft section was caught by the gooseneck wire and then pulled back into the left subclavian artery. The carrying wire and the traction wire were manipulated to properly position the aortic and branched graft sections.

After unfolding the graft, the aortic section and the branched section of the graft were dilated by a compliant balloon. The balloon was custom made and inserted via the introducer sheath. We did not use hypotension to place the graft or for balloon inflation. The carrying wire and the traction wires prevented migration of the stent graft during balloon inflation.

The sheath was removed, and the incision was closed. Fig 3 shows a successful implantation. Detailed information concerning the implantation techniques is available in previous reports.[7,8]

Follow-up protocol. All patients were examined with contrast enhanced helical CT scans before hospital discharge. The scans were repeated every 6 months. The mean follow-up period was 26 months (range, 7 to 65 months).

RESULTS

The stent grafts were successfully delivered and deployed in all patients. The mean procedure time, measured from the incision of the skin to surgical closure of the femoral access site, was 219 ± 68 minutes. The mean contrast media used in the procedures was 249 ± 99 mL.

All patients were transferred immediately to the ward without staying in the intensive care unit. Four patients required a blood transfusion. Major complications, defined as that caused any persistent disorders, occurred in one patient. The patient developed paraparesis that was probably caused by the accidental embolization of the Adamkiewicz artery. The graft of the patient was too short to cover the location of the Adamkiewicz artery, and the preprocedural images showed irregular, shaggy mural thrombus in the thoracic aorta.

Three access site complications occurred: a lymphorrhea, a pseudoaneurysm, and an intimal injury of the iliac artery. The lymphorrhea was resolved without aspiration. The pseudoaneurysm was successfully repaired by surgery. The intimal injury required a metallic stent implantation in the iliac artery. The three patients with minor complications were discharged without any disorders.

Complete exclusion of the inlet of the aneurysm or the primary entry tear of the aortic dissection at the time of the first postoperative CT scan was achieved in 14 patients

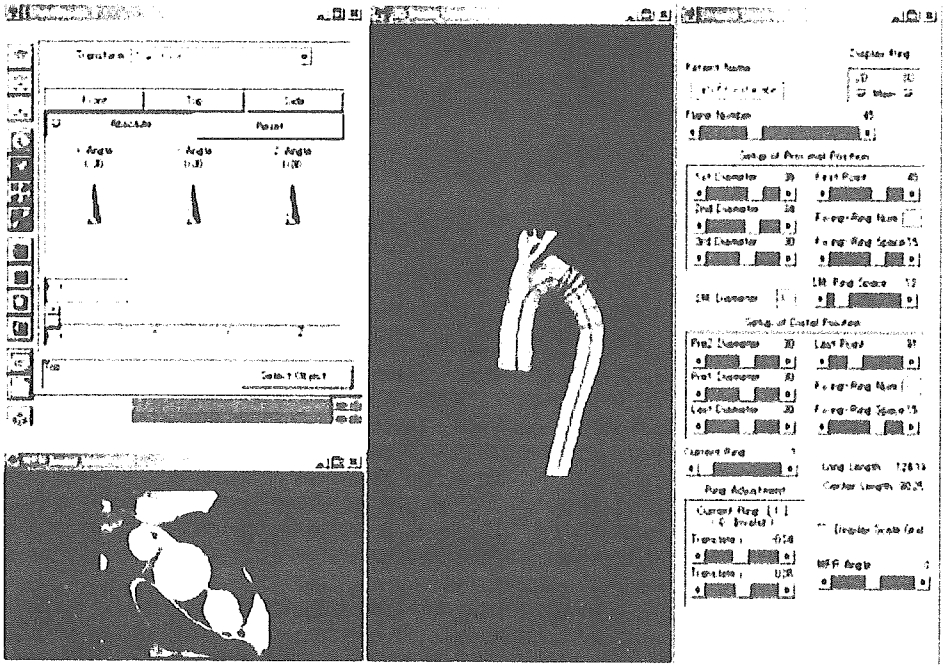

Fig 2. Monitor display of the computer program used to design the Inoue stent graft.

(82%). Attachment site endoleaks were revealed in three patients; two leaks were from the proximal attachment sites, and one leak was from the distal attachment site. The cause of the two endoleaks in the proximal attachment sites was considered unrelated to the branched section; they were instead considered caused by difficulties in implanting the stent graft in a curved position. The primary endoleak rate was 18%.

The average hospital stay after the procedure was 19 ± 27 days (range, 2 to 120). The patient who developed paraparesis required a distinctly prolonged hospital stay of 120 days for rehabilitation. All patients were discharged alive, and the 30-day mortality was 0%.

The mean follow-up period was 26 months (range, 7 to 65 months). More than a 3-mm sac size change was defined significant. Significant sac size shrinkage was achieved in 8 patients (47%). Sac size change was measured at the most recently obtained CT scan. Two of the three patients with attachment site endoleaks at the first postoperative CT scan required secondary stent grafting; one patient required implantation of a straight stent graft at the distal attachment site; the other patient required implantation of a double-branched stent graft.

Another patient with attachment site endoleak had a history of cerebral infarction, which occurred during previous open surgical replacement of a thoracoabdominal aortic aneurysm. We estimated that the risk of a repeat open surgery or secondary stent grafting procedure outweighed the risk of rupture. The aneurysmal sac size of the patient has not changed for 28 months.

Enlargement of the aneurysmal sac or secondary endoleak requiring secondary intervention has not been revealed in any of the other patients. CT scan confirmed that the branched section of the stent graft was patent in all cases. No stent graft migration occurred in any patient.

Two deaths occurred in the follow-up period. The cause of death was cerebral bleeding and pneumonia, both considered unrelated to the stent grafting. The initial and follow-up results are summarized in Table II.

DISCUSSION

Endovascular repair of thoracic aortic aneurysms may reduce morbidity and mortality.[2,3] The procedure is considered most suitable when the proximal end of the aneurysm is 1 to 2 cm from the left subclavian artery. Implantation can be difficult when the landing zone distal to the left subclavian artery is not sufficient.

Several options have been proposed to overcome this problem. The most traditional is prophylactic transposition or bypass graft placement to provide flow to the arm.[9-11] Some recent reports have described the safety of the intentional occlusion of the left subclavian artery by the stent graft without prophylactic surgical transposition. If arm, hand, or cerebral symptoms develop after coverage of the left subclavian artery, surgical revascularization of the subclavian artery is performed.[12-14] Although the early results of this option suggest that it is safe in most patients, some patients require transposition of the left subclavian artery in the follow-up.

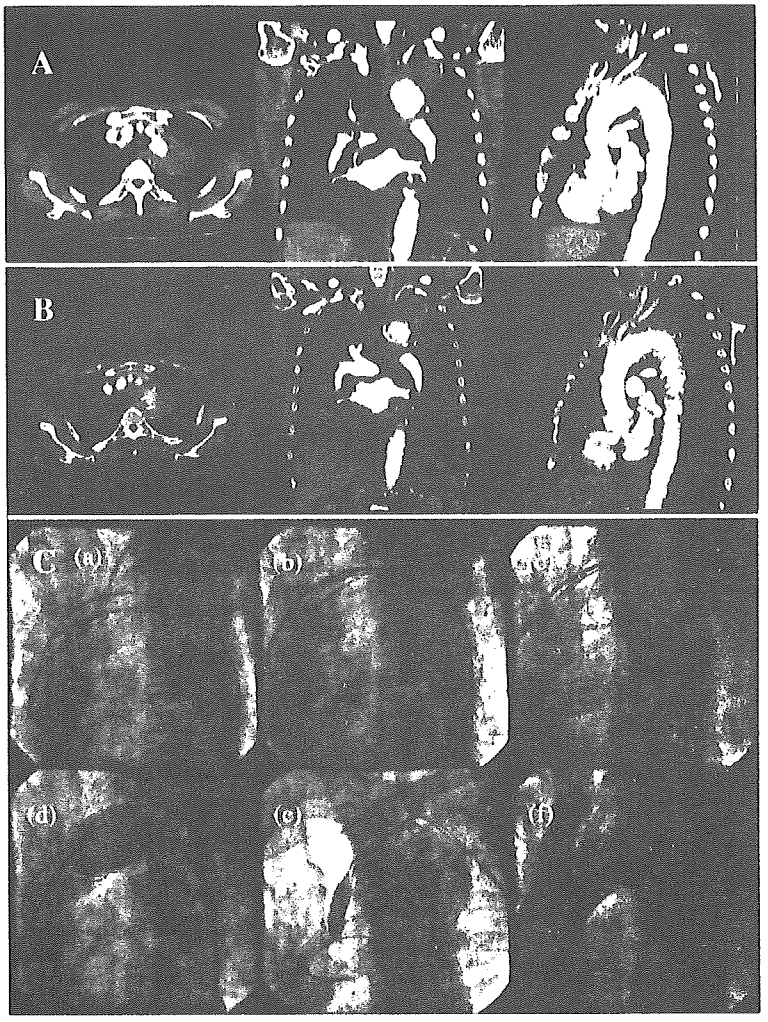

Fig 3. The successful implantation of the Inoue single-branched stent graft is shown for patient 16 in Table I. **A**, Enhanced computed tomography (CT) scan before treatment. **B**, Enhanced CT after treatment. **C**, Angiogram during the procedure. *a*, The folded Inoue stent-graft was delivered and positioned. *b*, The distal part of the aortic section of the graft was unfolded. *c*, After unfolding the proximal part of the aortic section of the graft, the distal neck was dilated. *d*, The proximal part of the aortic section was dilated. *e*, The branched section was dilated. *f*, The final angiogram revealed complete exclusion of the aneurysm.

Tiesenhausen et al[14] reported on eight patients who underwent thoracic aortic stent grafting without revascularizations of the left subclavian arteries. No immediate neurologic deficit or left arm ischemia occurred, but three patients required surgical revascularization of the left subclavian artery during follow-up. Furthermore, the occluded subclavian artery poses another problem: it may be a potential source of retrograde inflow into the excluded aneurysms or the false lumen.

Another option is to cross the origin of the left subclavian artery with the uncovered lesion of the stent graft.[15] The Talent LPS stent graft (Medtronic AVE, Santa Rosa, Calif) is usually used in this option. This option has limitations, however. The uncovered proximal stent aids in anchoring—not sealing—and leaks may occur. The uncovered stent may erode through the aorta.

Our option is to provide a stent graft with a side branch to the left subclavian artery.[7,8] This method does not require surgical transposition of the left subclavian artery and is widely applicable. However, except for the Inoue stent grafts, reports of endovascular techniques of complex aneurysm repair with branched stent grafts have been limited to animal studies and incidental case reports.[16,17]

In their initial experience with the branched stent-graft implantations, Inoue and colleagues[8] reported embolic cerebrovascular accident as the major complication. We consider that the risk of cerebral infarction is very low in the placement of a stent graft with a side branch to the left subclavian artery.

Table II. Initial and follow-up results of the patients. Corresponding patients' numbers are shown in Table I.

Patients	*Etiology*	*Hospital stay (day)*	*Complication*	*Endoleak at the first postoperative CT scan*	*Follow-up period (month)*	*Event in the follow-up period*
No. 1	Degenerative	19	No	No	65	Sac size stable
No. 2	Aneurysmal degeneration of a long standing aortic dissection	7	No	Yes (from the distal attachment site)	9	Sac size increased Secondary stent-grafting
No. 3	Chronic aortic dissection	4	No	No	54	Sac size reduced
No. 4	Chronic aortic dissection	3	No	No	53	Sac size reduced
No. 5	Aneurysmal degeneration of a long standing aortic dissection	3	No	No	50	Sac size stable
No. 6	Chronic aortic dissection	2	No	Yes (from the proximal attachment site)	35	Sac size increased Secondary stent-grafting
No. 7	Degenerative	26	Pseudoaneurysm	No	14	Sac size stable Death (cerebral bleeding)
No. 8	Degenerative	120	Paraparesis	No	9	Sac size stable Death (pneumonia)
No. 9	Chronic aortic dissection	8	No	No	35	Sac size reduced
No. 10	Degenerative	21	No	Yes (from the proximal attachment site)	28	Sac size stable
No. 11	Degenerative	29	Lymphorrhea	No	21	Sac size stable
No. 12	Acute aortic dissection	19	No	No	17	Sac size reduced
No. 13	Degenerative	13	No	No	17	Sac size reduced
No. 14	Degenerative	17	No	No	14	Sac size reduced
No. 15	Degenerative	14	No	No	13	Sac size stable
No. 16	Degenerative	10	No	No	9	Sac size reduced
No. 17	Ductus diverticulum	16	Intimal injury of the iliac artery	No	7	Sac size reduced

CT, computed tomography.

In normal human anatomy, the right common carotid artery and the right subclavian artery branch from the brachiocephalic artery, whereas the left common carotid artery and the left subclavian artery branch from the aorta directly. The right subclavian artery involves the common carotid artery, but the left subclavian artery does not. Thus, the single-branched stent-graft implantation is much safer than the double- or triple-branched stent-graft implantation in terms of the risk of cerebral infarction.

No cerebrovascular embolic events occurred in this study. Branched stent-graft implantation does not require surgical transposition of the left subclavian artery. Furthermore, this method offers another advantage: it may prevent the migration of the graft. Concerns about stent-graft migration in the long term have been reported.[18] Migration is associated with late aneurysm rupture, proximal endoleak, and graft kinking. The Inoue stent graft has no barbs to hold it in place. The branched section secures the proximal fixation and prevents later migration of the graft.

Our data suggest the feasibility of the single-branched stent-graft implantation for thoracic aorta. The Inoue single-branched stent graft offers an alternative mode of management for thoracic aortic aneurysms that involve the left subclavian artery and may expand the indication of thoracic stent grafting.

We thank M. Sato, ME and Y. Nagata, ME for their technical assistance.

REFERENCES

1. Okita Y, Ando M, Minatoya K, Tagusari O, Kitamura S, Nakajjma N, et al. Early and long-term results of surgery for aneurysms of the thoracic aorta in septuagenarians and octogenarians. Eur J Cardiothorac Surg 1999;16(3):317-23.
2. Dake MD, Miller DC, Semba CP, Mitchell RS, Walker PJ, Liddell RP. Transluminal placement of endovascular stent-grafts for the treatment of descending thoracic aortic aneurysms. N Engl J Med 1994;331(26): 1729-34.
3. Dake MD, Kato N, Mitchell RS, Semba CP, Razavi MK, Shimono T, et al. Endovascular stent-graft placement for the treatment of acute aortic dissection. N Engl J Med 1999;340(20):1546-52.
4. Leurs LJ, Bell R, Degrieck Y, Thomas S, Hobo R, Lundbom J. Endovascular treatment of thoracic aortic diseases: combined experience from the EUROSTAR and United Kingdom Thoracic Endograft registries. J Vasc Surg 2004;40(4):670-9; discussion 679-80.
5. Thurnher SA, Grabenwoger M. Endovascular treatment of thoracic aortic aneurysms: a review. Eur Radiol 2002;12(6):1370-87.
6. Imai Y, Urayama S, Uyama C, Inoue K, Ueno K, Kuribayashi S, et al. A system for computer-assisted design of stent grafts for aortic aneurysms using 3-D morphological models. Cardiovasc Intervent Radiol 2001; 24(4):277-9.
7. Inoue K, Sato M, Iwase T, Yoshida Y, Tanaka T, Tamaki S, et al. Clinical endovascular placement of branched graft for type B aortic dissection. J Thorac Cardiovasc Surg 1996;112(4):1111-3.
8. Inoue K, Hosokawa H, Iwase T, Sato M, Yoshida Y, Ueno K, et al. Aortic arch reconstruction by transluminally placed endovascular branched stent graft. Circulation 1999;100(19 Suppl):II316-21.
9. Shigemura N, Kato M, Kuratani T, Funakoshi Y, Kaneko M. New operative method for acute type B dissection: left carotid artery-left subclavian artery bypass combined with endovascular stent graft implantation. J Thorac Cardiovasc Surg 2000;120(2):406-8.

10. Heijmen RH, Deblier IG, Moll FL, Dossche KM, van den Berg JC, Overtoom TT, et al. Endovascular stent-grafting for descending thoracic aortic aneurysms. Eur J Cardiothorac Surg 2002;21(1):5-9.
11. Grabenwoger M, Hutschala D, Ehrlich MP, Cartes Zumelzu F, Thurnher S, Lammer J, et al. Thoracic aortic aneurysms: treatment with endovascular self-expandable stent grafts. Ann Thorac Surg 2000;69(2):441-5.
12. Gorich J, Asquan Y, Seifarth H, Kramer S, Kapfer X, Orend KH, et al. Initial experience with intentional stent graft coverage of the subclavian artery during endovascular thoracic aortic repairs. J Endovasc Ther 2002;9 Suppl 2:II39-43.
13. Hausegger KA, Oberwalder P, Tiesenhausen K, Tauss J, Stanger O, Schedlbauer P, et al. Intentional left subclavian artery occlusion by thoracic aortic stent grafts without surgical transposition. J Endovasc Ther 2001;8(5):472-6.
14. Tiesenhausen K, Hausegger KA, Oberwalder P, Mahla E, Tomka M, Allmayer T, et al. Left subclavian artery management in endovascular repair of thoracic aortic aneurysms and aortic dissections. J Card Surg 2003;18(5):429-35.
15. Burks JA Jr, Faries PL, Gravereaux EC, Hollier LH, Marin ML. Endovascular repair of thoracic aortic aneurysms: stent graft fixation across the aortic arch vessels. Ann Vasc Surg 2002;16(1):24-8.
16. Chuter TA, Schneider DB, Reilly LM, Lobo EP, Messina LM. Modular branched stent graft for endovascular repair of aortic arch aneurysm and dissection. J Vasc Surg 2003;38(4):859-63.
17. Vos AW, Linsen MA, Wisselink W, Ramwerda JA. Endovascular grafting of complex aortic aneurysms with a modular side branch stent graft system in a porcine model. Eur J Vasc Endovasc Surg 2004;27(5):492-7.
18. Resch T, Koul B, Dias NV, Lindblad B, Ivancev K. Changes in aneurysm morphology and stent graft configuration after endovascular repair of aneurysms of the descending thoracic aorta. J Thorac Cardiovasc Surg 2001;122(1):47-52.

Submitted Sep 19, 2004; accepted Nov 18, 2004.

INVITED COMMENTARY

Timothy A. M. Chuter, MD, *San Francisco, Calif*

In the accompanying paper, Saito et al describe their use of the Inoue system, a novel prosthesis with a side branch to the left subclavian artery, to achieve promising results in 17 cases of distal aortic arch repair. The Inoue system has several unusual features that lend themselves to this particular application:

- A supporting framework of nickel titanium rings confers great flexibility and is capable of sealing within a very short attachment site between the left subclavian and left carotid arteries.
- A corset of diameter-restricting ties allows final adjustments in the orientation and position of the unsheathed, but still constrained, prosthesis, as the subclavian side-branch is retrieved using a transbrachial snare and drawn all the way into the subclavian artery.
- Once deployed, the fully embedded unibody side branch has less effect on proximal aortic implantation than a conventional (external) modular attachment cuff that would have to remain within the aorta.

Their results show that the technique appears to be both safe and effective in the short-to-medium term: serious complications were rare, aneurysm dilatation was rare, and most type I endoleaks were treatable by endovascular means. Yet, it is too early to say that this approach is clearly better than the endovascular alternatives.

The attachment means is one cause for concern. Unbarbed nickel titanium rings have not generally been effective in preventing late-occurring migration and type I endoleak. An oversized ring buckles, distorts the profile of the attached graft orifice, and induces dilatation of the surrounding aorta, whereas an undersized ring exerts no outward force and produces neither seal nor resistance to migration. The stated 2% oversizing used by Inoue et al contains no margin for error. Perhaps the side branch of the Inoue device helps secure stent-graft position, but it would help more if it had the stiffness of a stent rather than the flexibility of a series of rings.

Stroke is notably absent from the current report. In previous reports, endovascular repair of the distal arch has often been complicated by embolic stroke, and multibranched versions of the current system are no exception. The current single-branched version requires less manipulation but does not altogether avoid instrumentation of the ascending aorta and arch. I suspect this system could still produce a high stroke rate in less experienced hands, which together with the high cost of customized device manufacture, would impede widespread application.

The most widely practiced alternative involves stent-graft coverage of the subclavian artery origin. Some provision for subclavian flow must be made in any patient with an internal mammary coronary graft, a dominant left vertebral artery, a high risk of paraplegia (distal thoracic aortic aneurysm or dissection), subclavian steal, or left arm claudication. I remain to be convinced that the single side-branch is superior to carotid-subclavian bypass or transposition.

Histone Acetyltransferase Activity of p300 Is Required for the Promotion of Left Ventricular Remodeling After Myocardial Infarction in Adult Mice In Vivo

Shoichi Miyamoto, MD*; Teruhisa Kawamura, MD, PhD*; Tatsuya Morimoto, MD, PhD; Koh Ono, MD, PhD; Hiromichi Wada, MD, PhD; Yosuke Kawase, PhD; Akira Matsumori, MD, PhD; Ryosuke Nishio, MD, PhD; Toru Kita, MD, PhD; Koji Hasegawa, MD, PhD

Background—Left ventricular (LV) remodeling after myocardial infarction is associated with hypertrophy of surviving myocytes and represents a major process that leads to heart failure. One of the intrinsic histone acetyltransferases, p300, serves as a coactivator of hypertrophy-responsive transcriptional factors such as a cardiac zinc finger protein GATA-4 and is involved in its hypertrophic stimulus-induced acetylation and DNA binding. However, the role of p300-histone acetyltransferase activity in LV remodeling after myocardial infarction in vivo is unknown.

Methods and Results—To solve this problem, we have generated transgenic mice overexpressing intact p300 or mutant p300 in the heart. As the result of its 2–amino acid substitution in the p300-histone acetyltransferase domain, this mutant lost its histone acetyltransferase activity and was unable to activate GATA-4–dependent transcription. The two kinds of transgenic mice and the wild-type mice were subjected to myocardial infarction or sham operation at the age of 12 weeks. Intact p300 transgenic mice showed significantly more progressive LV dilation and diminished systolic function after myocardial infarction than wild-type mice, whereas mutant p300 transgenic mice did not show this.

Conclusions—These findings demonstrate that cardiac overexpression of p300 promotes LV remodeling after myocardial infarction in adult mice in vivo and that histone acetyltransferase activity of p300 is required for these processes. **(*Circulation*. 2006;113:679-690.)**

Key Words: hypertrophy ■ myocytes ■ signal transduction

Left ventricular (LV) remodeling after myocardial infarction (MI) consists of dynamic changes in ventricular heart. It has been reported that among patients with acute MI, 20% had heart failure at the time of hospital admission and 9% have development of heart failure thereafter.[1] The hospital death rates associated with heart failure are greater in the latter. Therefore, elucidating the mechanisms of LV remodeling after MI is of clinical importance. During LV remodeling, hypertrophy of each surviving myocyte occurs in proportion to infarct size.[2]

Clinical Perspective p 690

Hypertrophic stimuli initiate a number of subcellular signaling pathways, which finally reach the nuclei of cardiac myocytes and change the pattern of gene expression.[3,4] Transcription factors that mediate these changes include myocyte enhancing factor-2,[5] serum response factor,[6] AP-1,[7] and a zinc finger protein, GATA-4.[7,8] The involvement of multiple transcription factors in hypertrophic responses suggests that these factors are coordinately activated.

An adenovirus E1A-associated protein, p300, acts as a coactivator of these hypertrophy-responsive transcription factors. In addition, p300 serves as an intrinsic histone acetyltransferase (HAT) and promotes an active chromatin configuration.[9–11] p300 protein can also acetylate certain nonhistone proteins such as DNA-binding transcription factors.[11–14] Acetylation is emerging as a posttranslational modification that is essential for the regulation of transcription and that modifies transcription factor affinity for binding sites on DNA, stability, and/or nuclear localization. Our previous study demonstrated that p300 can induce the acetylation and DNA binding of GATA-4. During myocardial cell hypertrophy, the acetylated form of GATA-4 and its DNA binding markedly increase, concomitant with an increase in p300 expression. In addition, a dominant-negative form of p300 inhibits agonist-induced

Received April 20, 2005; de novo received August 26, 2005; revision received October 17, 2005; accepted November 22, 2005.

From the Department of Cardiovascular Medicine, Graduate School of Medicine, Kyoto University, Kyoto, Japan (S.M., T.M., A.M., R.N., T. Kita); the Division of Translational Research, Kyoto Medical Center, National Hospital Organization, Kyoto, Japan (T. Kawamura, K.O., H.W., K.H.); and the Chugai Research Institute for Medical Science, Inc, Pharmacology & Pathology Research Center, Shizuoka, Japan (Y.K.).

*Drs Miyamoto and Kawamura contributed equally to this work.

Correspondence to Dr Koji Hasegawa, Division of Translational Research, Kyoto Medical Center, National Hospital Organization, 1-1 Mukaihata-cho, Fukakusa, Fushimi-ku, Kyoto, 612-8555, Japan. E-mail koj@kuhp.kyoto-u.ac.jp

Circulation is available at http://www.circulationaha.org

DOI: 10.1161/CIRCULATIONAHA.105.585182

hypertrophy, demonstrating a critical role of p300 in hypertrophic responses in cardiac myocytes in culture.[15] However, the precise role of p300 HAT activity in LV remodeling after MI in vivo is unknown. The present study was performed to solve this problem.

Methods

Plasmid Constructs

The expression vectors pcDNAG4, pCMVβ-gal, pCMVwtp300, and pCMVHATmutp300 contain the cytomegalovirus promoter/enhancer fused to cDNA encoding murine GATA-4,[16,17] β-galactosidase, a full-length human intact p300, or mutant p300, in which double amino acid substitution mutations were introduced,[18,19] respectively. pCMVwtp300 and pCMVHATmutp300 were gifts from Dr Richard Eckner, University of Medicine and Dentistry of NJ. The reporter plasmid pANF-luc consists of the firefly luciferase (luc) cDNA driven by a 131-bp rat atrial natriuretic factor (ANF) promoter sequence.[20] pET-1-CAT contains the transcription start site-proximal 204 bp of the wild-type (WT) rat endothelin-1 (ET-1) promoter fused to a bacterial chloramphenicol acetyltransferase (CAT) gene.[15] pRSVCAT and pRSVluc contain a bacterial CAT and a firefly luc gene, respectively, driven by Rous sarcoma virus (RSV) long terminal repeat sequences.[8]

Analysis of the Acetylation State of GATA-4 and Western Blotting

Cell culture of COS7 cells, immunoprecipitation, and Western blotting for acetylated lysine and GATA-4 were performed as previously described.[15] We used goat anti–GATA-4 polyclonal antibody (Santa Cruz Biotechnology) for immunoprecipitation, and rabbit polyclonal antibody against acetylated lysine (Cell Signaling), rabbit anti–GATA-4 polyclonal antibody (Santa Cruz Biotechnology), mouse anti-p300 monoclonal antibody (Upstate Biotechnology), mouse anti–β-actin monoclonal antibody (SIGMA), and mouse anti-GAPDH monoclonal antibody (Molecular Probes) for Western blotting. The level of acetylated GATA-4 was also analyzed by pulse-labeling as previously described.[15]

Electrophoretic Mobility Shift Assays

Electrophoretic mobility shift assays (EMSAs), with the GATA-4 site in the rat ET-1 promoter used as a probe, were carried out as previously described.[20] We also used a double-stranded oligonucleotide containing the Sp-1 binding site as a control probe (Santa Cruz Biotechnology).

Transfection and Luciferase/CAT Assays

COS7 cells were transfected with the indicated amounts of plasmid DNA through the use of LIPOFECTAMINE (Life Technologies, Inc), as previously described.[20] The relative luc or CAT activities in the same cell lysates were measured as described previously.[20]

Creation of Transgenic Mice

All animal experimental protocols were approved by the Institute of Laboratory Animals, Graduate School of Medicine, Kyoto University. Transgenic (Tg) mice overexpressing HATmut p300 (HATmut p300-Tg mice) in the heart were created as previously described.[15] Briefly, the α-myosin heavy chain (MHC)-HATmutp300 DNA plasmid was constructed by subcloning the *NotI-HindIII* fragment of pCMVHATmutp300 into the *SalI-HindIII* site of a 5.5-kb mouse α-MHC promoter–containing construct. The α-MHC-HATmutp300 DNA fragment was gel-purified and injected into newly fertilized C57BL/6 oocytes, which were transferred to the oviducts of pseudopregnant C57BL/6 recipients. All animals were maintained under specific pathogen-free conditions.

Experimental MI and Physiological Studies

All mice used in the present study were female. Mice were anesthetized with 1.0 to 1.5% isoflurane, and open-chest coronary artery ligation was performed. MI was induced by ligating the left anterior descending coronary artery. In sham-operated mice, the suture was passed but not tied. Five weeks after the operation, we noninvasively measured heart rate and blood pressure with a photoelectric pulse device (UR-5000, Ueda Production Corp) placed on the tail of prewarmed mice. We then performed echocardiography under anesthesia with 2.5% avertin. Transthoracic echocardiography was performed with a cardiac ultrasound recorder (Philips Sonos 5500), using a 12-MHz transducer. For cardiac catheterization, mice were anesthetized with a mixture of ketamine (100 mg/kg) and xylazine (5 mg/kg) intraperitoneally. The pressure-volume loops and intracardiac ECG were monitored online, and the conductance, pressure, and intracardiac electrocardiographic signals were digitized at 2 kHz, stored on disk, and analyzed as previously described.[21]

Histological Analysis

After the physiological analysis, all surviving mice were euthanized, and their hearts were removed. The excised hearts were cut into 2 transverse slices at the mid level of the papillary muscles; the basal specimens were fixed in 10% buffered formalin and embedded in paraffin, after which 4-μm-thick sections were stained with hematoxylin and eosin, Masson trichrome, and sirius red CI 35870 (0.05% solution in saturated aqueous picric acid). Quantitative assessments of infarct size, noninfarct size, cross-sectional myocardial cell diameter, cell populations, and fibrotic area were performed on 20 randomly chosen high-power fields in each section with the use of Axioskop 2 FS plus (Zeiss).

Measurement of Myocardial ET-1 Levels

ET-1 was extracted from the supernatant of homogenized LV tissues and measured by means of the sandwich enzyme immunoassay, as previously described.[22]

Statistical Analysis

Data are presented as mean±SD. Statistical comparisons were performed with the use of unpaired 2-tailed Student *t* tests or ANOVA with Scheffé test where appropriate, with a probability value <0.05 taken to indicate significance. The log-rank test was used to evaluate survival rate.

Results

HAT Activity of p300 Is Required for Acetylation and DNA Binding of GATA-4

To determine the role of p300 HAT activity in acetylation and DNA binding of GATA-4, we performed experiments using pCMVHATmutp300, an expression plasmid encoding mutant p300 (HATmut p300). We performed immunoprecipitation/Western blotting in COS7 cells transfected with pcDNAG4 in the presence or absence of pCMVwtp300 or pCMVHATmutp300. No protein was immunoprecipitated with control IgG (Figure 1A, lane 4). Forced expression of intact p300 induced acetylation of GATA-4, whereas expression of HATmut p300 did not induce acetylation (Figure 1A, upper panel). GATA-4 was similarly immunoprecipitated with anti–GATA-4 antibody in the 3 groups (Figure 1A, lower panel). Before immunoprecipitation, the expression levels of GATA-4 were similar in the 3 groups (Figure 1B, middle panel). Furthermore, intact p300 and HATmut p300 were expressed at similar levels (Figure 1B, upper panel). We also performed pulse-labeling experiments. Incorporation of sodium [^{14}C]acetate into GATA-4 protein was clearly detected in pCMVwtp300-transfected cells but not in pCMVHATmutp300-

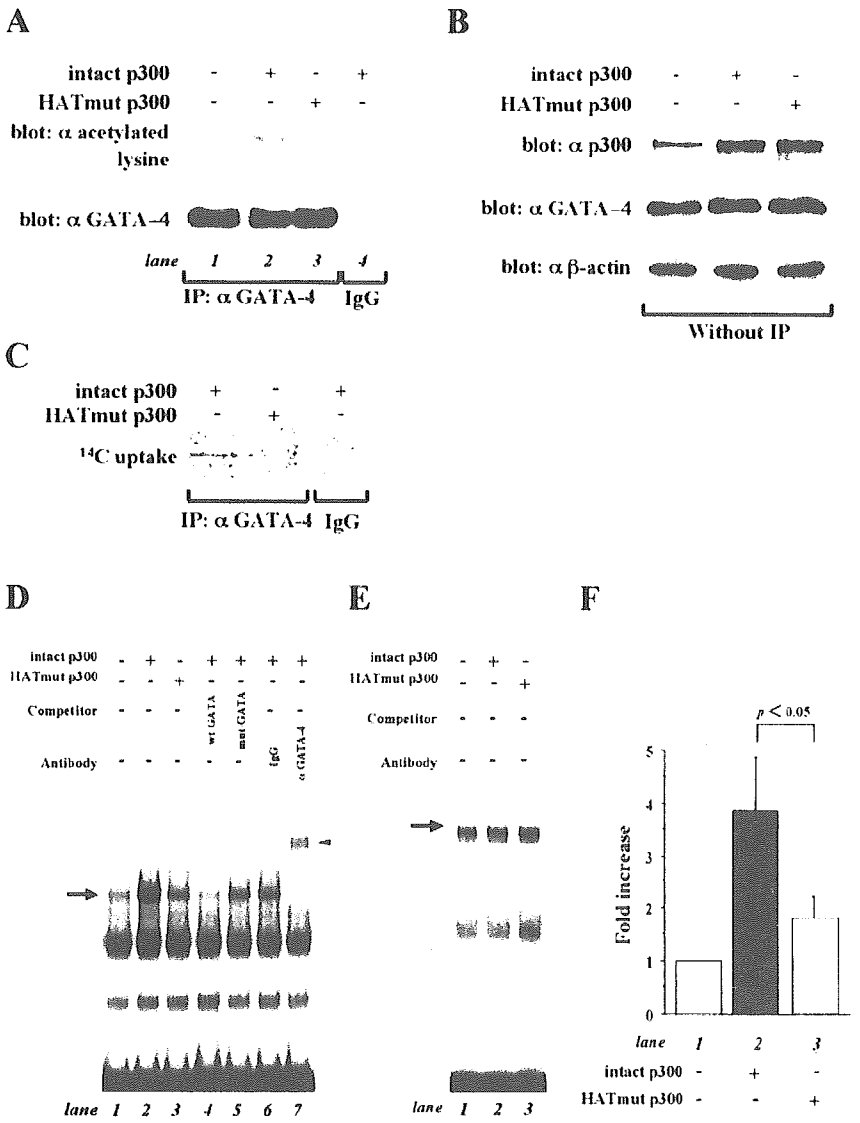

Figure 1. Histone acetyltransferase (HAT) activity of p300 is required for acetylation and DNA binding of GATA-4. A, COS7 cells were transfected with 2 μg of pcDNAG4 in the presence or the absence of pCMVwtp300 (10 μg) or pCMVmutp300 (10 μg), as indicated. The total amount of DNA was kept constant by cotransfecting pCMVβ-gal. Protein extracts from these cells were immunoprecipitated with goat anti-GATA-4 polyclonal antibody, followed by sequential Western blotting with rabbit antiacetylated lysine polyclonal antibody and with rabbit anti-GATA-4 polyclonal antibody. B, The extracts used in A before immunoprecipitation were subjected to Western blotting with the use of antibodies against p300, GATA-4, and β-actin. C, COS7 cells were transfected with 2 μg of pcDNAG4 in addition to 10 μg of pCMVwtp300 or pCMVmutp300 and were pulse-labeled with [^{14}C] acetic acid, sodium salt for 3 hours. The protein extracts were immunoprecipitated with goat anti-GATA-4 polyclonal antibody or with normal goat IgG and resolved by SDS-PAGE. D and E, The same extracts used in A and B were probed with a radiolabeled double-stranded oligonucleotide containing the GATA-4 site in the ET-1 promoter (D) and with one containing the Sp-1 site (E). F, The amount of GATA-4/DNA binding (indicated by an arrow) was quantified by densitometry with the use of NIH image 1.61.

transfected ones (Figure 1C). Next, the same extracts used in the experiments shown in Figure 1, A and B, were subjected to EMSAs by using the GATA-4 site of ET-1 promoter as a probe (Figure 1D). Competition and supershift experiments demonstrated that the retarded band (indicated by an arrow) represents an interaction of the probe with GATA-4. Notably, expression of intact p300 markedly increased GATA-4/DNA binding (lane 2) compared with β-gal expression (lane 1), whereas that of mutant p300 only modestly increased (lane 3, Figure 1, D and F). Sp-1/DNA binding was similar among the 3 groups (Figure 1E). These findings demonstrate that the HAT activity of p300 plays a critical role in acetylation and DNA binding of GATA-4.

HAT Activity of p300 Is Required for Synergistic Activation of GATA-4–Dependent Promoters

To examine whether the HAT activity of p300 participates in GATA-4–dependent transcription of the ET-1 and ANF genes, we performed transient transfection experiments. As shown in Figure 2, A and B, transfection of either pcDNAG4 (lane 2), pCMVwtp300 (lane 3), or pCMVHATmutp300 (lane 5) alone resulted in only modest increases in ANF and ET-1 promoter activities. Transfection of pCMVwtp300 in addition to pGATA-4 (lane 4) induced a marked activation of these promoter activities. However, transfection of pCMVHATmutp300 only modestly augmented GATA-4–dependent ET-1 or ANF transcription (lane 6). Intact p300 and HATmutant p300 were similarly expressed in extracts from pCMVwtp300-transfected and pCMVHATmutp300-transfected cells (Figure 2C, upper panel, lanes 3 to 6). GATA-4 levels were also similar among lanes 2, 4, and 6 (Figure 2C, middle panel). These findings demonstrate that p300 and GATA-4 synergistically activate the ANF and ET-1 promoters and that the HAT activity of p300 is required for these activations.

HAT Activity of p300 Is Required for Acetylation of GATA-4 in the Mouse Heart

To further investigate the role of p300 HAT activity in LV remodeling after MI in vivo, we generated Tg mice

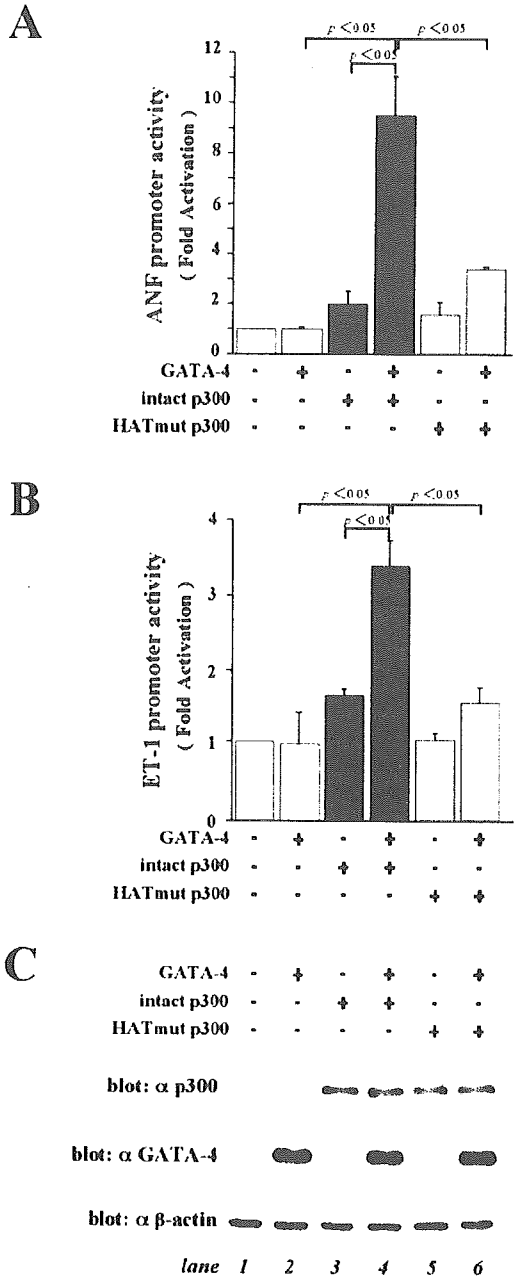

Figure 2. Histone acetyltransferase (HAT) activity of p300 participates in GATA-4–dependent activation of atrial natriuretic factor (ANF) and endothelin-1 (ET-1) promoters. A and B, COS7 cells were transfected with 2.0 μg of pANF-luc and 0.1 μg of pRSV-CAT (A) or 2.0 μg of pET-1-CAT and 0.1 μg of pRSV-luc (B) in the presence or absence of 0.5 μg of pcDNAG4 and 2.5 μg of pCMVwtp300 or pCMVmutp300, as indicated. The total amount of DNA was kept constant by cotransfecting pCMVβ-gal. The results, expressed as fold induction of reporter constructs, are mean±SD of 3 independent experiments, each carried out in duplicate. C, Extracts from these cells were subjected to Western blotting for p300, GATA-4, and β-actin.

overexpressing intact p300 or HATmut p300 in the heart. Among multiple lines we obtained, we selected two independent lines for each type of Tg mouse (intact p300-Tg: lines 21 and 39; HATmut p300-Tg: lines 17 and 23) because the expression levels of the transgene in the heart were similar among these four lines. Since similar findings were obtained for the two lines in each kind of Tg mice, we show in the present study combined data of these two lines.

At the age of 12 weeks, cardiac function and morphology of each type of Tg mice were similar to those of the corresponding WT mice. These mice were then subjected to either sham operation or MI operation. Five weeks later, extracts from the whole LV except for the scar area of these mice were subjected to Western blotting with anti-p300 antibody that recognized the proteins produced from both transgenes (intact p300 and HATmut p300) as well as endogenous p300 (Figure 3A, upper panel, and Figure 3B). In the sham operation groups, intact p300- and HATmut p300-Tg mouse hearts showed an 8-fold increase in total p300 content, compared with their corresponding WT mouse hearts (compare lanes 1 and 3 and lanes 5 and 7 in Figure 3B). Endogenous p300 levels in WT mouse hearts increased after MI (compare lanes 1 and 2 and lanes 5 and 6 in Figure 3B). However, in the hearts of intact p300-Tg and HATmut p300-Tg mice, total p300 levels were similar between the sham operation and MI groups (compare lanes 3 and 4 and lanes 7 and 8 in Figure 3B). On the other hand, the total amounts of cardiac GATA-4 were similar in all groups (Figure 3A, middle panel).

Next, we investigated the role of p300 HAT activity in GATA-4 acetylation in mouse hearts. Signals of acetylated GATA-4 (Figure 3C, upper panel) were distinct in intact p300-Tg mice (lanes 3 and 4) but undetectable or very weak in WT mice (lanes 1 and 2) and HATmut p300-Tg mice (lanes 5 and 6). In all kinds of mice, the signals were higher in the MI groups than in the sham-operated groups. GATA-4 was similarly immunoprecipitated with anti–GATA-4 antibody in all these groups (Figure 3C, lower panels, lanes 1 to 6). No protein was immunoprecipitated with control IgG (lanes 7 and 8). These findings demonstrate that the overexpression of p300 in the heart promotes the acetylation of GATA-4 and that the HAT activity of p300 is required for this effect.

Cardiac Overexpression of Intact p300 but Not of Mutant p300 Augments LV Remodeling After MI

All sham-operated mice survived throughout the study. We next examined the mortality of MI-operated mice after the operation. Mortality at day 0, which indicates acute surgical death due to MI, did not differ among WT, intact p300-Tg, and HATmut p300-Tg mice (Figure 4A). The 5-week survival rate was significantly lower in intact p300-Tg mice than the corresponding WT mice but was similar between HATmut p300-Tg and WT mice. Autopsy revealed considerable pleural effusion and pulmonary congestion in almost all of the mice that died later than 2 days after MI, suggesting that these mice predominantly died of heart failure. Compared with HATmut p300-Tg mice, the mortality rate of intact p300-Tg mice was remarkably increased later than 2 days after MI. Thus, this increase may come from increased incidence of heart failure in intact p300-Tg mice after MI.

Next, we performed physiological study to evaluate cardiac morphological and functional changes at 5 weeks

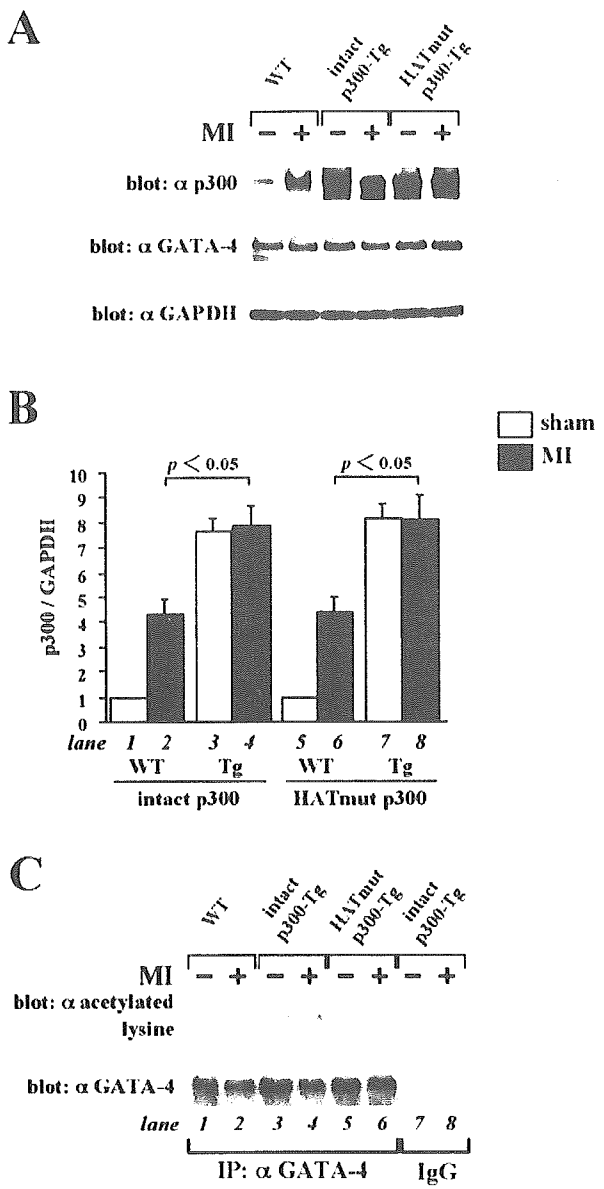

Figure 3. Histone acetyltransferase (HAT) activity of p300 is required for acetylation of GATA-4 in adult mouse hearts. A and B, Five weeks after the sham or MI operation, 10 μg of protein extracts from WT and intact p300- or HATmut p300-Tg mouse hearts were subjected to Western blotting with anti-p300 antibody, anti–GATA-4 antibody, or anti-GAPDH antibody. Representative photographs in each group are shown (A). The levels of signals were quantified, and results from 6 animals in each group are expressed as mean±SD (B). C, Protein extracts from WT and intact p300- or HATmut p300-Tg mouse hearts were immunoprecipitated with goat anti–GATA-4 polyclonal antibody or control goat IgG and sequentially subjected to Western blotting for acetylated lysine and GATA-4.

after sham or MI operation. Echocardiographic data in the sham-operation groups was similar among all kinds of mice (WT, intact p300-Tg, and HATmut p300-Tg). After MI, however, increase in LV end-diastolic and end-systolic dimension and decrease in percent fractional shortening were more prominent in intact p300-Tg than WT mice but were similar between WT and HATmut p300-Tg mice (Figure 4, B and C). Systolic and diastolic blood pressures were similar among these kinds of mice. Cardiac catheterization data (Figure 5) in the sham operation groups were also similar among all kinds of mice except for LV end-diastolic pressure, LV end-systolic volume, and τ, the time constant of isovolumic relaxation, which were slightly increased in intact p300-Tg mice. After MI, the increases in LV end-diastolic volume (LVEDV), LV end-systolic volume, and LV end-diastolic pressure and the decreases in normalized end-systolic volume elastance (NL Ees) and preload recruitable volume work were more prominent in intact p300-Tg than their corresponding WT mice but were similar between HATmut p300-Tg and their WT mice. In summary, diastolic function is impaired in intact p300-Tg mice compared with other kinds of mice. In addition, in accord with the data obtained by echocardiography, MI-induced changes, consisting of decreased contractility, chamber dilation, and low output, were more prominent in intact p300-Tg mice than in HATmut p300-Tg or WT mice.

Consistent with the findings of the physiological analysis, histological analysis at 5 weeks after MI revealed a severely dilated LV cavity with a thin infarct wall in intact p300-Tg mice compared with HATmut p300-Tg or WT mice (Figure 6A). The absolute infarct size was similar among the different kinds of mice, whereas the noninfarct area was modestly increased in intact p300-Tg mice (Figure 6B). There was no significant difference in percentages of infarct area relative to total LV area among WT (23.4%), intact p300-Tg (21.3%), and HATmut p300-Tg (22.1%) mice, suggesting that severe LV remodeling in intact p300-Tg mice developed independent of infarct size in these mice. In addition, in the MI groups, LV cavity area (Figure 6C) and heart weight/body weight ratio (Figure 6D) after MI were larger in intact p300-Tg than HATmur p300-Tg or WT mice.

Although there were no significant differences in histology among the different kinds of sham-operated mice, cross-sectional myocardial cell diameter at 5 weeks after MI was larger in intact p300-Tg mice than in WT or HATmut p300-Tg mice (Figure 7, A and B). In the MI groups, the population of noncardiomyocytes in the infarct area (Figure 7C) and the amount of fibrosis in the infarct area (Figure 7D) and in the noninfarcted LV walls (Figure 7E) were similar among WT, intact p300-Tg, and HATmut p300-Tg mice. These findings demonstrate that p300 promotes MI-induced LV remodeling associated with the hypertrophy of individual myocytes and that the HAT activity of p300 is required for this promotion.

HAT Activity of Cardiac p300 Is Involved in Increase in GATA-4/DNA binding and LV ET-1 Expression After MI

To examine changes in GATA-4/DNA-binding after MI in WT, intact p300-Tg, and HATmut p300-Tg mouse hearts, EMSAs using the ET-1 GATA site as a probe were performed in cardiac nuclear extracts from these mice 5 weeks after the operation. Competition and supershift experiments demonstrated that the retarded band (indicated by an arrow) represents an interaction of the probe with cardiac GATA-4

A

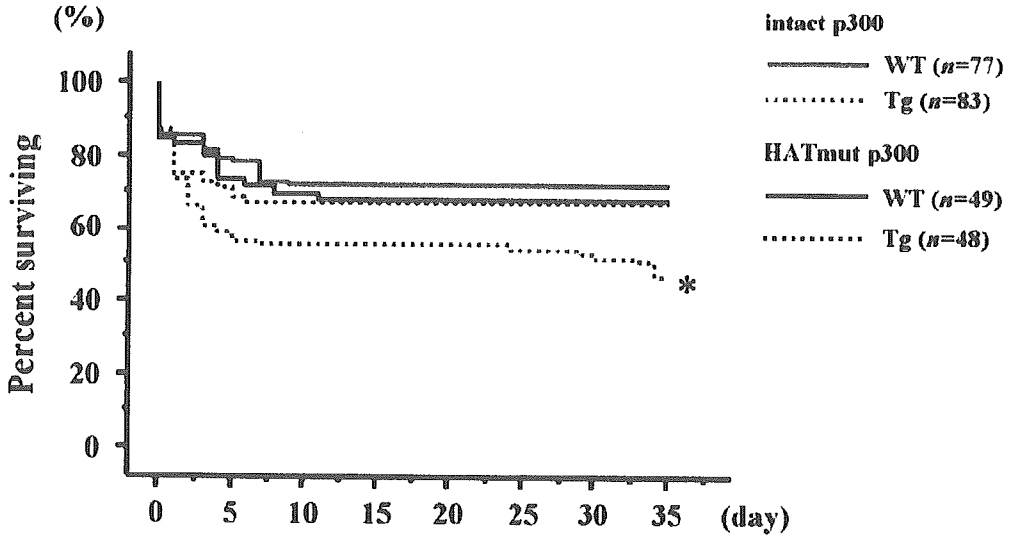

* $p < 0.05$ vs WT and HATmut p300 Tg

B

	intact p300				HATmut p300			
	WT		Tg		WT		Tg	
MI	(-)	(+)	(-)	(+)	(-)	(+)	(-)	(+)
	n=15	n=21	n=17	n=18	n=16	n=23	n=21	n=16
HR (bpm)	443 ± 47	456 ± 90	441 ± 30	425 ± 39	468 ± 49	476 ± 63	475 ± 37	460 ± 42
systole BP (mmHG)	118 ± 10	117 ± 10	116 ± 9	114 ± 10	124 ± 13	123 ± 13	122 ± 9	114 ±12
diastole BP (mmHG)	51 ± 9	52 ± 10	53 ± 14	55 ± 11	60 ± 11	60 ± 11	58 ± 12	53 ±8
LVEDD (mm)	3.57 ± 0.22	4.43 ± 0.39 †	3.74 ± 0.25	5.41 ± 0.51 *¶	3.41 ± 0.11	4.31 ± 0.20 †	3.63 ± 0.23	4.39 ± 0.37 #
LVESD (mm)	1.90 ± 0.26	3.20 ± 0.51 †	2.03 ± 0.20	4.55 ± 0.68 *¶	1.86 ± 0.27	3.16 ± 0.27 †	1.98 ± 0.24	3.21 ± 0.47 #
FS (%)	46.9 ± 4.50	28.0 ± 7.60 †	45.6 ± 3.40	16.3 ± 6.30 *¶	45.6 ± 7.10	26.6 ± 4.80 †	45.5 ± 5.50	27.1 ± 5.90 #

†$p<0.05$ versus corresponding WT MI(-) *$p<0.05$ versus intact p300-Tg MI(-)
¶ $p<0.05$ versus HATmut p300-Tg MI(+) #$p<0.05$ versus HATmut p300-Tg MI(-)

C

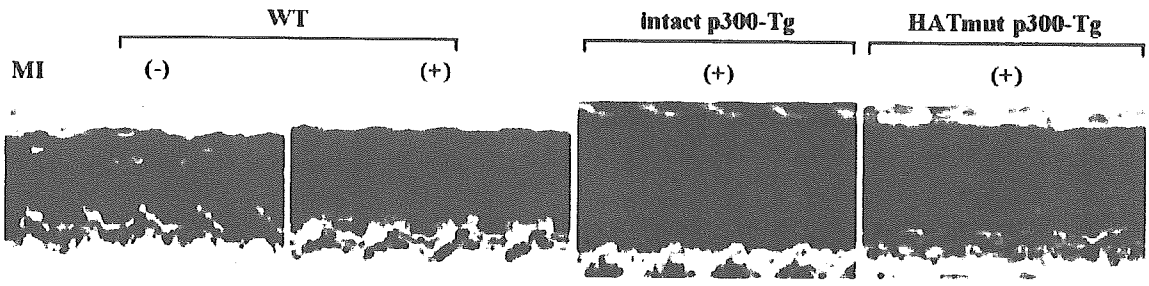

Figure 4. Survival rates and echocardiography data after MI. At the age of 12 weeks, intact p300-Tg mice, their corresponding WT mice, HATmut p300-Tg mice, and their corresponding WT mice were subjected to sham or MI operation. A, Kaplan-Meier survival curves of MI-operated mice. B, Echocardiographic data at 5 weeks after sham or MI operation. HR indicates heart rate; BP, blood pressure; LVEDD, left ventricular chamber diameter in end-diastole; LVESD, left ventricular chamber diameter in end-systole; FS, fractional shortening. C, Representative photographs of M-mode images.

(Figure 8A). GATA-4/DNA binding in the heart was increased after MI in each kind of mouse. In the MI groups, however, the intensity of GATA-4/DNA binding was significantly higher in intact p300-Tg than in WT mice but was similar between HATmut p300-Tg and WT mice (Figure 8, B and C). In contrast, cardiac Sp-1 binding activities were similar among all kinds of mice (Figure 8D). Finally, we measured LV levels of ET-1, a downstream target of the

A

	intact p300				HATmut p300			
	WT		Tg		WT		Tg	
MI	(-)	(+)	(-)	(+)	(-)	(+)	(-)	(+)
	n=7	n=3	n=5	n=5	n=3	n=3	n=3	n=3
HR (min⁻¹)	392 ± 11	405 ± 46	392 ± 25	374 ± 11	425 ± 25	438 ± 36	429 ± 22	429 ± 19
ESP (mmHg)	96.1 ± 6.1	88.5 ± 14.4	91.2 ± 4.5	83.4 ± 5.3	93.8 ± 6.7	90.0 ± 9.7	101.7 ± 7.4	94.7 ±5.6
EDP (mmHg)	1.8 ± 0.4	4.9 ± 0.5	4.9 ± 0.7	15.3 ± 2.5 ‡*¶	4.1 ± 0.5	7.1 ± 1.4	3.4 ± 2.2	9.4 ±2.5
ESV (μL)	7.5 ± 0.8	27.5 ± 6.1 †	13.5 ± 2.0	94.3 ± 18.8 ‡*¶	8.7 ± 1.3	25.3 ± 3.8 †	9.7 ± 3.2	26.3 ± 2.9 #
EDV (μL)	19.2 ± 1.6	36.2 ± 10.7 *	25.7 ± 1.7	98.6 ± 18.4 ‡*¶	23.9 ± 3.2	34.1 ± 4.9	27.6 ± 2.3	32.6 ± 4.8
SI (μL/g)	0.58 ± 0.07	0.42 ± 0.15	0.59 ± 0.11	0.19 ± 0.08 *	0.73 ± 0.13	0.40 ± 0.06	0.82 ± 0.11	0.28 ± 0.08 #
EF (%)	59.8 ± 4.3	24.4 ± 7.1 †	47.1 ± 6.8	4.7 ± 2.4 ‡*¶	63.7 ± 2.4	26.1 ± 2.4 †	65.7 ± 9.6	18.1 ± 4.3 #
CI (μL/min g)	230 ± 33	156 ± 41	234 ± 53	69 ± 31 *	314 ± 70	179 ± 37	355 ± 62	121 ±39 #
dP/dtmax (mmHg/s)	8388 ± 1324	7049 ± 2231	7266 ± 1029	3612 ± 473	7708 ± 240	6219 ± 2385	8542 ± 235	6114 ±822
dP/dtmin (mmHg/s)	5200 ± 737	4644 ± 1124	3691 ± 92	1935 ± 156 ‡*	5132 ± 117	5096 ± 1054	6309 ± 890	3780 ± 514
τ (ms)	9.3 ± 0.7	10.6 ± 2.2	14.3 ± 0.6 †	24.0 ± 2.9 ‡¶	9.1 ± 1.5	12.4 ± 0.7	9.4 ± 0.9	12.5 ± 0.3
NL Ees (mmHg/μL · 100mg)	16.80 ± 4.57	8.45 ± 2.69 †	11.26 ± 1.60	2.73 ± 1.18 *	12.71 ± 1.05	6.95 ± 0.70 †	12.22 ± 0.39	6.97 ± 0.81 #
NL Eed (mmHg/μL · 100mg)	0.39 ± 0.12	0.66 ± 0.12	0.37 ± 0.07	1.45 ± 0.12 ‡*	0.45 ± 0.21	0.74 ± 0.15	0.25 ± 0.17	1.59 ± 0.47 #
PRSW (mmHg)	70.0 ± 6.3	50.1 ± 7.5 †	62.9 ± 4.6	28.3 ± 5.9 ‡*¶	69.5 ± 4.6	39.5 ± 13.6 †	58.9 ± 11.7	40.5 ±2.4

†$p<0.05$ versus corresponding WT MI(-) ‡$p<0.05$ versus corresponding WT MI(+) *$p<0.05$ versus intact p300-Tg MI(-)
¶ $p<0.05$ versus HATmut p300-Tg MI(+) #$p<0.05$ versus HATmut p300-Tg MI(-)

B

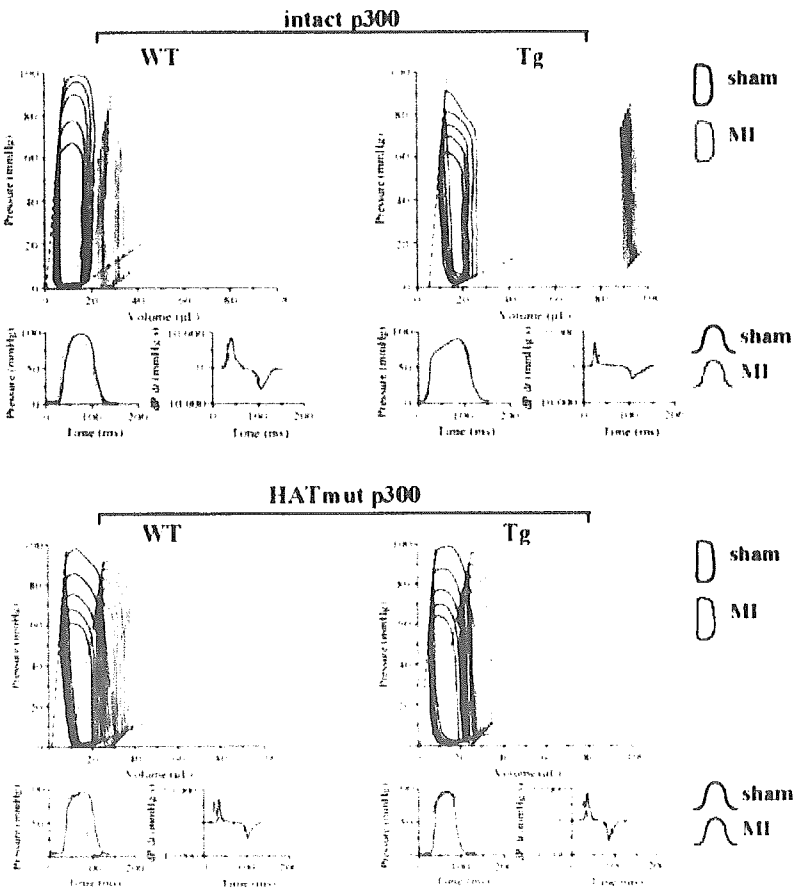

Figure 5. Hemodynamics of Tg and WT mouse hearts after MI. Five weeks after sham or MI operation, hemodynamics of Tg mice and their WT mice were examined as described in the Methods section. A, Values represent mean ± SEM of 3 to 7 mice in each group, as indicated. ESP indicates end-systolic pressure; EDP, end-diastolic pressure; ESV, end-systolic volume; EDV, end-diastolic volume; SI, stroke volume index; CI, cardiac index; dP/dtmax, maximum derivative of change in systolic pressure over time; dP/dtmin, minimum derivative of change in diastolic pressure over time; τ, time constant of isovolumic relaxation; NL Ees, normalized end-systolic volume elastance; NL Eed, normalized end-diastolic volume elastance; PRSW, preload recruitable volume work. B, Representative curves of pressure-volume relations, LV pressure, and slope of derivative of change in systolic pressure over time (dP/dt) in sham versus MI.

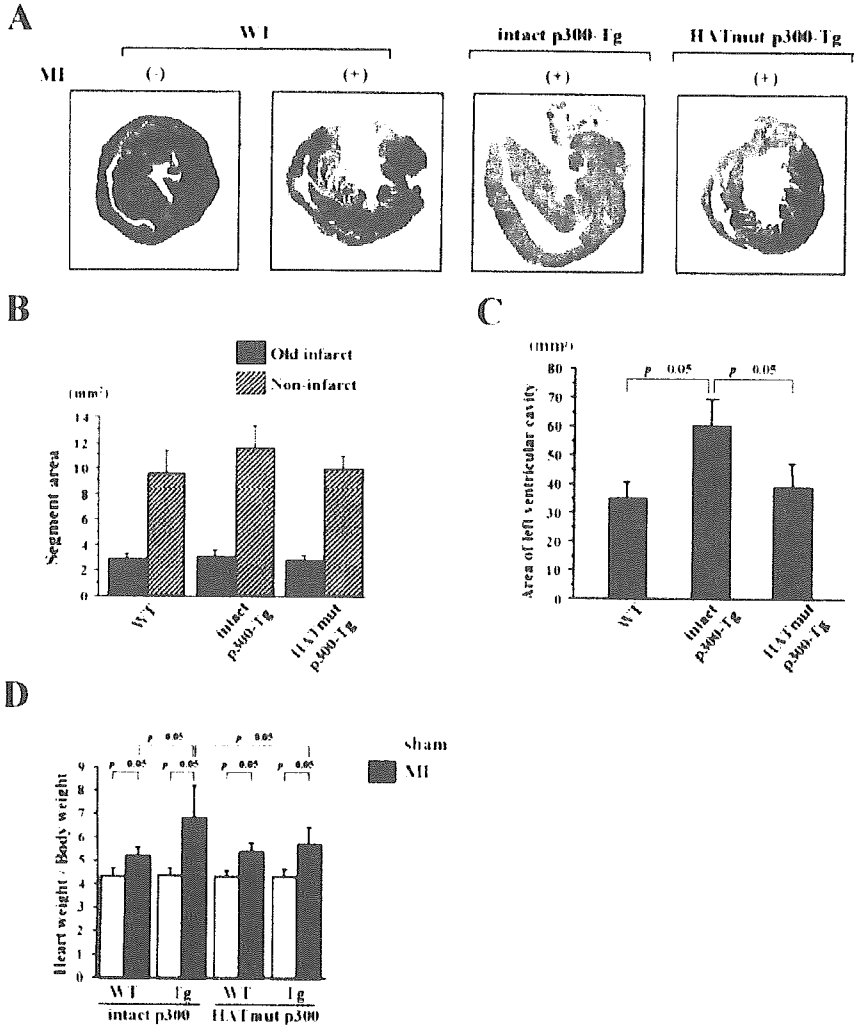

Figure 6. Morphology of Tg and WT mouse hearts after MI. A through C, Transverse sections of mouse hearts at 5 weeks after sham or MI operation were stained with Masson trichrome. A, Representative photographs. B and C, Areas of old infarct and noninfarct and those of LV cavity were measured. Results from 7 animals in each group are expressed as mean±SD. D, Results of heart weight (mg)/body weight (g) ratio from more than 20 animals in each group are expressed as mean±SD.

p300/GATA-4 pathway (Figure 8E). Although LV ET-1 levels in the sham operation groups did not differ among WT, intact p300-, and HATmut p300-Tg mice, the levels were increased after MI in each kind of mouse. Consistent with the findings of EMSAs, the LV ET-1 levels in the MI groups were higher in intact p300-Tg than HATmut p300-Tg mice. These findings suggest that the HAT activity of p300 is involved in the MI-induced increase in the LV ET-1 level as well as GATA-4/DNA binding.

Discussion

The present study investigated the role of p300 HAT activity in LV remodeling after MI in vivo. The HAT domain of p300 has been mapped previously to residues 1284 to 1669.[18] p300 HAT activity is able to acetylate not only histone tails but also transcriptional regulators such as p53 or p300 itself.[11–14] HATmut p300, a mutant we used in the present study, was almost completely defective in histone-p53 acetylation and autoacetylation.[18] In agreement with these findings, HATmut p300 was unable to induce acetylation or DNA binding of GATA-4 in adult mouse hearts as well as in vitro, although acetylation of other components of the transcriptional machinery might be affected in the heart of HATmut p300-Tg. However, HATmut p300 did not act as a transcriptional repressor but had modest ability to enhance GATA-4–dependent transcription. These findings suggest that HATmut p300 acts as a silent mutant and not as a dominant-negative mutant. Three cysteine-histidine–rich domains, which are important in mediating protein-protein interaction, are conserved in HATmut p300. Therefore, the bridging function of HATmut p300 will be conserved in this mutant and might be involved in the modest activation of GATA-4–dependent transcription.

The present study demonstrated that acetylation of GATA-4 in WT hearts increased after MI, concomitant with an increase in expression of endogenous p300. Thus, p300 may be one of the factors that mediate the acetylation during LV remodeling. However, acetylation and DNA binding of GATA-4 in Tg mouse hearts increased after MI even without an increase in the total p300 content. During myocardial cell hypertrophy, activation of mitogen-activated protein kinases induces p300 phosphorylation, which results in enhanced p300 HAT activity.[23,24] Thus, such modification of p300 as well as changes of its quantity might regulate the acetylation of GATA-4 during LV remodeling after MI. It is also possible that other HATs

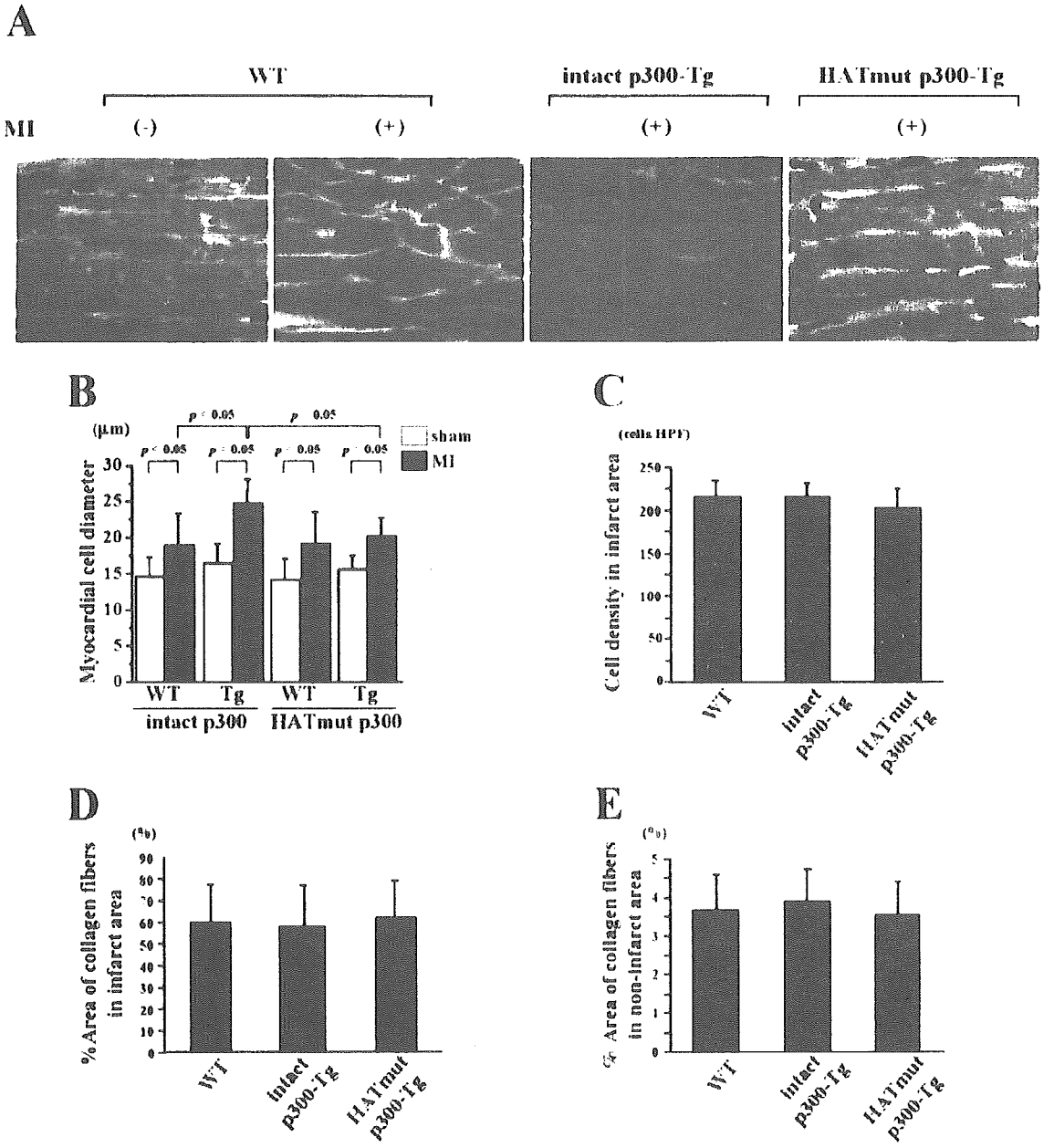

Figure 7. Histological analysis of Tg and WT mouse hearts after MI. A through E, Five weeks after sham or MI operation, histological sections of mouse hearts were subjected to hematoxylin and eosin staining (A through C) or sirius red staining (D and E). A, Representative photographs at magnification ×400. B, The average of 50 individual myocardial cell diameters were calculated for 1 animal, and results from 5 animals in each group are expressed as mean ± SD. C, Cell density in infarcted area was measured in each group. D and E, Percentage of areas taken up by collagen fibers in either infarcted (D) or noninfarcted (E) region. Results from 7 animals in each group are expressed as mean ± SD (C through E).

such as p300/CBP associating factor (P/CAF) play a role in MI-induced acetylation. In addition, acetylation of nuclear proteins is regulated by histone deacetylases.[25] Therefore, to clarify the precise mechanisms of acetylation during LV remodeling after MI, it would be interesting to examine the association of GATA-4 or myocyte enhancing factor-2 with p300 and histone deacetylases during this process.

In the absence of MI, activation of p300 alone in female mice does not lead to increase in heart size or increased mortality rates at the age of 17 weeks or younger. However, LV remodeling after MI was more exaggerated in intact p300-Tg mice than in HATmut p300-Tg mice. In close association with LV remodeling, acetylation and DNA binding of GATA-4 in the MI group were higher in intact p300-Tg mice than in HATmut p300-Tg mice. The LV level of ET-1, a downstream target of GATA-4, revealed a similar tendency to its DNA binding. These findings demonstrate that a sufficient level of p300 HAT activity is critical for the acetylation and DNA binding of GATA-4 and for promotion of LV remodeling after MI in adult mice in vivo. Interestingly, despite the overexpression of p300, interstitial cell proliferation and fibrosis

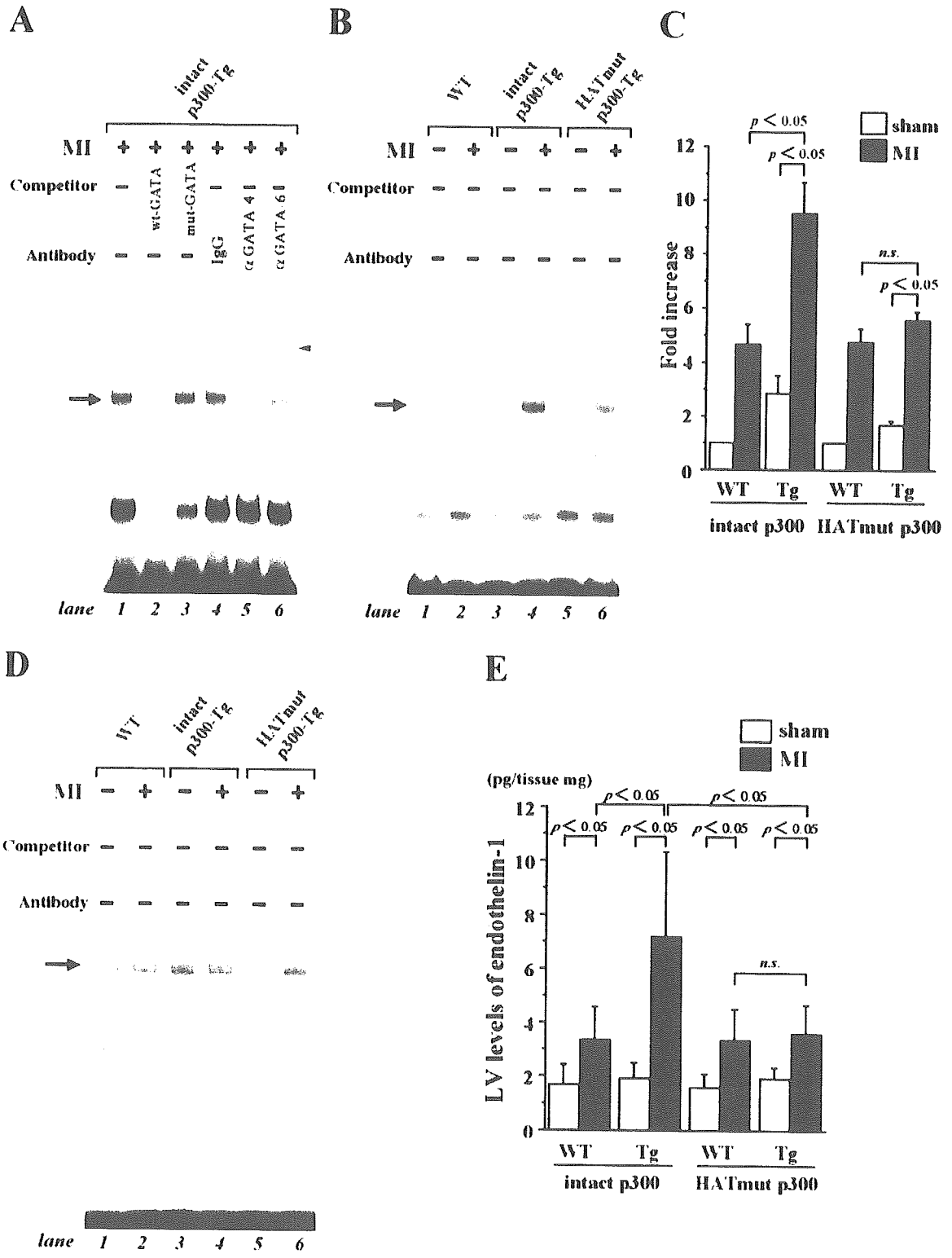

Figure 8. GATA-4/DNA binding and endothelin-1 (ET-1) level after MI in Tg and WT mouse hearts. A, Five weeks after sham or MI operation, 10 μg of protein extracts from mouse hearts were probed with a radiolabeled double-stranded oligonucleotide containing the GATA site in the ET-1 promoter. Unlabeled competitor DNAs were present at a 100-fold molar excess where indicated: lane 2, a wild-type GATA oligonucleotide (*WT-GATA*); lane 3, a mutant GATA oligonucleotide (*Mut-GATA*). Supershift assays were performed in the presence of 4 μg of control IgG, anti–GATA-4 antibody, or anti–GATA-6 antibody, as indicated (lanes 4 to 6). B and C, The amount of GATA-4/DNA binding (indicated by an arrow) was compared among extracts from each group. Representative photograph (B) and quantitative data (C) are shown. The relative amount of DNA binding in the hearts of sham-operated WT mice was set at 1.0. Values are mean ± SD of 6 animals in each group. D, The same extracts used for (B) and (C) were also probed with radiolabeled double-stranded oligonucleotide containing the Sp-1 site. E, Results of LV ET-1 levels from more than 10 animals in each group are expressed as mean ± SD.

remain unaffected, whereas interstitial cell proliferation is an important feature of LV remodeling. However, individual myocyte growth was remarkable in intact p300-Tg mouse hearts compared with WT mouse hearts. This observation suggests that p300 augments post-MI remodeling by affecting growth of each myocyte.

Recent studies suggest that GATA-6 as well as GATA-4 is involved in the hypertrophic response in cardiac myocytes.[26] By supershift experiments, the present study demonstrated that GATA-6 is not a major GATA factor contained in cardiac nuclear complex formed with ET-1 GATA site (Figure 8A). However, these data do not rule out the possible redundant and compensative roles of GATA-6 during LV remodeling after MI. In addition, p300 is able to interact not only with GATA-4[15,20] but also with other hypertrophy-responsive transcription factors such as myocyte enhancing factor-2,[27] nuclear factor of activated T-lymphocyte,[28] and AP-1.[29] Our findings might be applicable to these factors as well. The present study suggests that HAT activity of p300 could be a pharmacological target for LV remodeling after MI in humans. Recently, a natural compound, anacardic acid, was shown to inhibit HAT activity.[30] Therefore, it would be interesting to test whether p300 HAT inhibitors can block MI-induced LV remodeling in vivo.

Acknowledgments

This work was supported in part by grants (to T.K. and K.H.) from the Ministry of Education, Science, and Culture of Japan. The authors thank N. Sowa and S. Nagata for excellent technical assistance.

Disclosures

None.

References

1. Spencer FA, Meyer TE, Gore JM, Goldberg RJ. Heterogeneity in the management and outcomes of patients with acute myocardial infarction complicated by heart failure: the National Registry of Myocardial Infarction. *Circulation*. 2002;105:2605–2610.
2. Rubin SA, Fishbein MC, Swan HJ. Compensatory hypertrophy in the heart after myocardial infarction in the rat. *J Am Coll Cardiol*. 1983; 1:1435–1441.
3. Chien KR, Zhu H, Knowlton KU, Miller-Hance W, van Bilsen M, O'Brien TX, Evans SM. Transcriptional regulation during cardiac growth and development. *Annu Rev Physiol*. 1993;55:77–95.
4. Sadoshima J, Izumo S. The cellular and molecular response of cardiac myocytes to mechanical stress. *Annu Rev Physiol*. 1997;59:551–571.
5. Kolodziejczyk SM, Wang L, Balazsi K, DeRepentigny Y, Kothary R, Megeney LA. MEF2 is upregulated during cardiac hypertrophy and is required for normal post-natal growth of the myocardium. *Curr Biol*. 1999;9:1203–1206.
6. Paradis P, MacLellan WR, Belaguli NS, Schwartz RJ, Schneider MD. Serum response factor mediates AP-1-dependent induction of the skeletal alpha-actin promoter in ventricular myocytes. *J Biol Chem*. 1996;275:10827–10833.
7. Herzig TC, Jobe SM, Aoki H, Molkentin JD, Cowley AW Jr, Izumo S, Markham BE. Angiotensin II type Ia receptor gene expression in the heart: AP-1 and GATA-4 participate in the response to pressure overload. *Proc Natl Acad Sci U S A*. 1997;94:7543–7548.
8. Hasegawa K, Lee SJ, Jobe SM, Markham BE, Kitsis RN. cis-Acting sequences that mediate induction of beta-myosin heavy chain gene expression during left ventricular hypertrophy due to aortic constriction. *Circulation*. 1997;96:3943–3953.
9. Ogryzko VV, Schiltz RL, Russanova V, Howard BH, Nakatani Y. The transcriptional coactivators p300 and CBP are histone acetyltransferases. *Cell*. 1996;87:953–959.
10. Hebbes TR, Thorne AW, Crane-Robinson C. A direct link between core histone acetylation and transcriptionally active chromatin. *EMBO J*. 1988;7:1395–1402.
11. Chan HM, La Thangue NB. p300/CBP proteins: HATs for transcriptional bridges and scaffolds. *J Cell Sci*. 2001;114:2363–2373.
12. Gu W, Roeder RG. Activation of p53 sequence-specific DNA binding by acetylation of the p53 C-terminal domain. *Cell*. 1997;90:595–606.
13. Lill NL, Grossman SR, Ginsberg D, DeCaprio J, Livingston DM. Binding and modulation of p53 by p300/CBP coactivators. *Nature*. 1997;387:823–827.
14. Imhof A, Yang XJ, Ogryzko VV, Nakatani Y, Wolffe AP, Ge H. Acetylation of general transcription factors by histone acetyltransferases. *Curr Biol*. 1997;7:689–692.
15. Yanazume T, Hasegawa K, Morimoto T, Kawamura T, Wada H, Matsumori A, Kawase Y, Hirai M, Kita T. Cardiac p300 is involved in myocyte growth with decompensated heart failure. *Mol Cell Biol*. 2003;23:3593–3606.
16. Arceci RJ, King AA, Simon MC, Orkin SH, Wilson DB. Mouse GATA-4: a retinoic acid-inducible GATA-binding transcription factor expressed in endodermally derived tissues and heart. *Mol Cell Biol*. 1993;13:2235–2246.
17. Ip HS, Wilson DB, Heikinheimo M, Tang Z, Ting CN, Simon MC, Leiden JM, Parmacek MS. The GATA-4 transcription factor transactivates the cardiac muscle-specific troponin C promoter-enhancer in nonmuscle cells. *Mol Cell Biol*. 1994;14:7517–7526.
18. Bordoli L, Husser S, Luthi U, Netsch M, Osmani H, Eckner R. Functional analysis of the p300 acetyltransferase domain: the PHD finger of p300 but not of CBP is dispensable for enzymatic activity. *Nucleic Acids Res*. 2001;29:4462–4471.
19. Eckner R, Ewen ME, Newsome D, Gerdes M, DeCarprio JA, Lawrence JB, Livingston DM. Molecular cloning and functional analysis of the adenovirus E1A-associated 300-kD protein (p300) reveals a protein with properties of a transcriptional adaptor. *Genes Dev*. 1994;8: 869–884.
20. Kakita T, Hasegawa K, Morimoto T, Kaburagi S, Wada H, Sasayama S. p300 protein as a coactivator of GATA-5 in the transcription of cardiac-restricted atrial natriuretic factor gene. *J Biol Chem*. 1999; 274:34096–34102.
21. Nishio R, Sasayama S, Matsumori A. Left ventricular pressure-volume relationship in a murine model of congestive heart failure due to acute viral myocarditis. *J Am Coll Cardiol*. 2002;40:1506–1514.
22. Iwanaga Y, Kihara Y, Hasegawa K, Inagaki K, Yoneda T, Kaburagi S, Araki M, Sasayama S. Cardiac endothelin-1 plays a critical role in the functional deterioration of left ventricles during the transition from compensatory hypertrophy to congestive heart failure in salt-sensitive hypertensive rats. *Circulation*. 1998;98:2065–2073.
23. Ait-Si-Ali S, Carlisi D, Ramirez S, Upegui-Gonzalez LC, Duquet A, Robin P, Rudkin B, Harel-Bellan A, Trouche D. Phosphorylation by p44 MAP kinase/ERK1 stimulates CBP histone acetyl transferase activity in vitro. *Biochem Biophys Res Commun*. 1999;262:157–162.
24. Gusterson RJ, Yuan LW, Latchman DS. Distinct serine residues in CBP and p300 are necessary for their activation by phenylephrine. *Int J Biochem Cel Biol*. 2004;36:893–899.
25. Vega RB, Harrison BC, Meadows E, Roberts CR, Papst PJ, Olson EN, McKinsey TA. Protein kinases C and D mediate agonist-dependent cardiac hypertrophy through nuclear export of histone deacetylase 5. *Mol Cell Biol*. 2004;24:8374–8385.
26. Liang Q, De Windt LJ, Witt SA, Kimball TR, Markham BE, Molkentin JD. The transcription factors GATA4 and GATA6 regulate cardiomyocyte hypertrophy in vitro and in vivo. *J Biol Chem*. 2001; 276:30245–30253.
27. Slepak TI, Webster KA, Zang J, Prentice H, O'Dowd A, Hicks MN, Bishopric NH. Control of cardiac-specific transcription by p300 through myocyte enhancer factor-2D. *J Biol Chem*. 2001;276: 7575–7585.
28. Kawamura T, Ono K, Morimoto T, Akao M, Iwai-Kanai E, Wada H, Sowa N, Kita T, Hasegawa K. Endothelin-1-dependent nuclear factor of activated T lymphocyte signaling associates with transcriptional coactivator p300 in the activation of the B cell leukemia-2 promoter in cardiac myocytes. *Circ Res*. 2004;94:1492–1499.
29. Yamashita K, Discher DJ, Hu J, Bishopric NH, Webster KA. Molecular regulation of the endothelin-1 gene by hypoxia: contri-

butions of hypoxia-inducible factor-1, activator protein-1, GATA-2, AND p300/CBP. *J Biol Chem*. 2001;276:12645–12653.
30. Davidson SM, Townsend PA, Carroll C, Yurek-George A, Balasubramanyam K, Kundu TK, Stephanou A, Packham G, Ganesan A, Latchman DS. The transcriptional coactivator p300 plays a critical role in the hypertrophic and protective pathways induced by phenylephrine in cardiac cells but is specific to the hypertrophic effect of urocortin. *Chembiochem*. 2005;6:162–170.

CLINICAL PERSPECTIVE

Left ventricular remodeling after MI consists of dynamic and biological changes of the heart. During LV remodeling, hypertrophy of each surviving myocyte occurs in proportion to infarct size and represents a major process that leads to heart failure. Hypertrophic stimuli initiate a number of subcellular signaling pathways, which finally reach the nuclei of cardiac myocytes and change the pattern of gene expression. To establish an efficient pharmacological therapy for LV remodeling, it is critical to identify a common nuclear target of hypertrophic stimuli in cardiac myocytes. One of the intrinsic histone acetyltransferases, p300, serves as a coactivator of hypertrophy-responsive transcriptional factors such as a cardiac zinc finger protein GATA-4 and is involved in its hypertrophic stimulus-induced acetylation and DNA binding. The present study demonstrates that cardiac p300 augments post-MI remodeling by affecting growth of each myocyte in adult mice in vivo. In addition, a sufficient level of p300 HAT activity was required for the acetylation and DNA binding of GATA-4 and for the promotion of LV remodeling after MI. These data suggest that HAT activity of p300 could be a pharmacological target for LV remodeling after MI in humans.

WTC deafness Kyoto (dfk): a rat model for extensive investigations of Kcnq1 functions

Hiroshi Gohma, Takashi Kuramoto, Mitsuru Kuwamura, Ryoko Okajima, Noriaki Tanimoto, Ken-ichi Yamasaki, Satoshi Nakanishi, Kazuhiro Kitada, Takeru Makiyama, Masaharu Akao, Toru Kita, Masashi Sasa and Tadao Serikawa

Physiol. Genomics 24:198-206, 2006. First published Dec 20, 2005;
doi:10.1152/physiolgenomics.00221.2005

Physiological Genomics publishes results of a wide variety of studies from human and from informative model systems with techniques linking genes and pathways to physiology, from prokaryotes to eukaryotes. It is published quarterly in January, April, July, and October by the American Physiological Society, 9650 Rockville Pike, Bethesda MD 20814-3991. Copyright © 2005 by the American Physiological Society. ISSN: 1094-8341, ESSN: 1531-2267. Visit our website at http://www.the-aps.org/.